Journal of the Korean Ceramic Society
Vol. 54, No. 1, pp. 43~48, 2017.

https://doi.org/10.4191/kcers.2017.54.1.06

Effect of Additive Size on the Densification and Thermal Conductivity of AlN Ceramics with MgO–CaO–Al_2O_3–SiO_2 Additives

Hwa-Jun Lee*,, Woo-Seok Cho*, Hyeong Jun Kim*, Hyung-Tae Kim*, and Sung-Soo Ryu*,†**

**Engineering Ceramic Center, Korea Institute of Ceramic Engineering and Technology, Icheon 17303, Korea*

***School of Advanced Materials Science and Engineering, Sungkyunkwan University, Suwon 16419, Korea*

(Received August 31, 2016; Revised October 26, November 8, 2016; Accepted November 8, 2016)

ABSTRACT

In this study, we investigate the effect of additive size on the densification and thermal conductivity of AlN ceramics with MgO–CaO–Al_2O_3–SiO_2 (MCAS) additives. Micro-sized MCAS powder prepared via melting and nano-sized MCAS powder synthesized via the polymeric complex method are used as sintering additives. We analyze the densification behavior of AlN added with 5 wt.% of MCAS by dilatometry as well as by isothermal sintering in the temperature range of 1300 ~ 1700°C. AlN exhibits higher sinterability with nano-MCAS than with micro-MCAS, and both specimens approach their maximum densities when sintered at 1600°C for 4 h. The thermal conductivities of AlN with 5 wt% of nano- and micro-MCAS additives sintered at 1600°C are 82.6 and 32.0 W/mK, respectively. We find that nano-MCAS is more effective in sintering of AlN ceramics at lower temperatures, and thus for enhancing their thermal conductivities.

Key words : AlN, Sintering additive, Densification, Thermal property

1. Introduction

Aluminum nitride (AlN) exhibits high thermal conductivity, low dielectric constant, high electrical resistivity, and a thermal expansion coefficient comparable to that of Si. These unique properties make it a promising material for use as a packaging substrate for high-power integrated circuits.[1-5] AlN is a strong, covalently-bonded material, which makes sintering very difficult. Full densification requires temperatures over 1900°C. In addition, the sintering atmosphere must be properly controlled to prevent oxidation at temperatures above 1000°C.

These issues have attracted significant interest in the development of finer AlN powders and additives such as alkaline-earth and rare-earth oxides to enable sintering at lower temperatures.[5-12] Komeya *et al.*[9,10] approached the issue systematically and reported that sintering additives such as $CaCO_3$, Y_2O_3, etc. are very effective in the pressureless sintering of AlN at 1800°C. These additives play two roles. First, they interact with the Al_2O_3 layer on the AlN surface to form liquid aluminates, enabling liquid-phase sintering. Second, they enhance the thermal conductivity by decreasing the dissolved oxygen content of the AlN lattice.

However, the aforementioned sintering temperature is very high. It increases manufacturing costs, and causes undesirable, exaggerated grain growth that adversely affects the mechanical properties of AlN. Furthermore, there are restrictions on the selection of metal electrodes for co-firing of AlN multilayer substrates. Thus, the densification of AlN at low temperatures has recently attracted significant interest.[13-18]

Troczynski and Nicholson densified AlN with 9 wt% of a CaO-Y_2O_3-SiO_2-La_2O_3-CeO_2 system at 1600°C.[13] Streicher *et al.*[14] also densified AlN to its maximum density with 0.5 wt% of $3CaO_3$-SiO_2-Al_2O_3 or $CaCO_3$ at 1650°C. Jarrige *et al.*[15] sintered AlN at 1600°C with 2 wt% of $12CaO_7$-Al_2O_3-Y_2O_3 or $12CaO_7$-Al_2O_3-$CaYAlO_4$, and achieved up to 97% of the theoretical density. Watari *et al.*[16] used the Y_2O_3-CaO-Li_2O system as a sintering additive and reported thermal conductivities of 100–172 W/mK for bodies sintered at 1600°C.

Liu *et al.* produced a densely-sintered AlN with CaF_2 and YF_3 at 1650°C, and reported a thermal conductivity of 187 W/mK.[17] Qiao *et al.* also synthesized a densely-sintered AlN with 2 wt% of CaF_2 and Y_2O_3 added at 1650°C, and reported a thermal conductivity of 148 W/mK.[18]

In addition to the cases above, there have been many recent studies of low-temperature sintering of AlN using additives made from glass ceramics with low melting temperatures.[19-21] For example, Yang *et al.*[21] prepared MgO–CaO–Al_2O_3–SiO_2 (MCAS) glass via a sol-gel method, and verified that it is an effective additive for the low temperature sintering of AlN. A previous study[22] demonstrated that 5 wt% of micro-sized MCAS glass prepared via melting causes AlN to densify at 1600°C. However, its thermal conductivity was 25 W/mK, which is much lower than with Y_2O_3 or CaO additives.

It is logical to reason that the particle size of the additive

†Corresponding author : Sung-Soo Ryu
E-mail : ssryu@kicet.re.kr
Tel : +82-31-645-1447 Fax : +82-31-645-1485

can play an important role on the sinterability and thermal conductivity of AlN. Some studies have reported that smaller particles provide better densification and thermal conductivities.[23,24] Qiao *et al.*[24] fully densified AlN at 1600ºC by incorporating 3.53 and 2.0 wt% of nano-sized Y_2O_3 and CaO additives, respectively. They reported that a significant enhancement in thermal conductivity is possible in this system. Lee *et al.*[25] recently confirmed that the polymeric complex method (PCM) can be used to synthesize nano-MCAS with particle sizes around 50 nm, and that the resulting nano-additive is very effective in the sintering of AlN at low temperatures.

In this study, we used the MCAS system as an additive for low-temperature sintering of AlN, and investigated the effect of its particle size on densification and thermal conductivity. We prepared two additives, a micro-sized MCAS powder via the melting method, and a nano-sized powder via the PCM.

2. Experimental Procedure

We used a commercial AlN powder (Grade H, Tokuyama, Japan) synthesized via carbothermal reduction and nitridation. Two additives, nano- and micro-sized MCAS were synthesized via melting and the PCM, respectively. We used a melting procedure described in a previous study.[22] First, the starting materials consisting of 5 wt% of MgO, 19 wt% of CaO, 26 wt% of Al_2O_3, and 50 wt% of SiO_2 were mixed in a ball mill, and the mixture was melted at 1500ºC. Next, the melt was quenched and dry-ground in a planetary mill to produce a fine powder.

We also performed the PCM using a procedure described in a previous study.[25] The starting materials were citric acid ($C_6H_8O_7$), ethylene glycol ($HOCH_2CH_2OH$), magnesium nitrate hexahydrate ($Mg(NO_3)_2$ $6H_2O$), calcium carbonate ($CaCO_3$), aluminum nitrate nonahydrate ($Al(NO_3)_3$ $9H_2O$), and tetraethyl orthosilicate ($C_8H_{20}O_4Si$). The concentrations were set to yield the same composition as produced via melting. First, a mixture of citric acid (CA) and ethylene glycol (EG) (CA : EG = 1 : 5 molar ratio) was prepared, and $Mg(NO_3)_2$, $CaCO_3$, $Al(NO_3)_3$, and $C_8H_{20}O_4Si$ were sequentially dissolved into the solution at 90ºC. The mixture was thermally polymerized at 300ºC and then at 400ºC for 5 h. This processing yielded a black solid. The solid was thermally treated again in air for 5 h at 700ºC, resulting in a nano-sized MCAS powder.

Figure 1 shows field emission scanning electron microscopy (FE-SEM) images of the two additives. The nano- and micro-sized MCAS comprise particles of about 50 nm and 5 μm, respectively. Fig. 2 is the particle-size distribution of the micro-sized MCAS, as determined via laser diffraction. It confirms an average particle size of about 5 μm.

For sintering experiments, AlN powder was mixed with 5 wt% of either MCAS additive in a mini mill (pulverisette 23, FRITSCH, Germany). The mixture was pressed in a super-alloy mold (10 mm diameter) at 20 MPa, then exposed

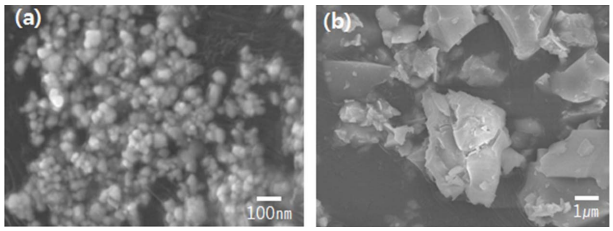

Fig. 1. SEM images of two types of MgO–CaO–Al_2O_3–SiO_2 (MCAS) powders used as the sintering additive for AlN ceramics; (a) polymerized complex method and (b) melt method.

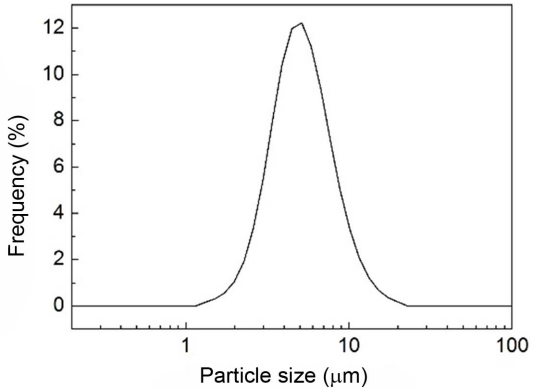

Fig. 2. Particle size distribution of the MCAS powder prepared by the melt method.

to cold isostatic pressing at 200 MPa, which produced disc-shaped green samples. Their sintering shrinkage was measured using a dilatometer (DIL-402C, Netzsch, Germany) by heating at a rate of 5ºC/min and holding at 1600ºC for 4 h.

Isothermal sintering was carried out in a sintering furnace (Thermvac, Korea) with a tungsten heating element. Samples were placed on a tungsten plate coated with BN powder, inside a tungsten crucible. The furnace pressure was reduced to 100 mTorr and nitrogen was introduced at a flow rate of 2 L/min. Then, the temperature was increased to a set point between 1300 and 1700ºC at a rate of 5ºC/min. Sintering proceeded at that temperature for 4 h.

The sintered density was measured via Archimedes' principle, and its microstructure was analyzed via FE-SEM (JSM-9701, JEOL, Japan). The crystalline phase of the sintered body was identified via X-ray diffraction (XRD, D/max-2500, RIGAKU, Japan) at 40 kV/200 mA, in the 2θ range of 10 - 80º, with a scan rate of 5º/min.

The sintered AlN disks were prepared via a typical procedure for thermal conductivity measurements, and tested using a laser flash analyzer (LFA447, NETZSCH, Germany) at 25ºC. We calculated the thermal conductivity (λ, mm^2/s) using the following equation:

$$\lambda(T) = \alpha(T) \times \rho(T) \times C_p(T) \quad (1)$$

Here, ρ(T): density (g/cm^3)

C_p: specific heat (J/g·K)

3. Results and Discussion

3.1. Shrinkage behavior

Figure 3(a) shows the linear shrinkage behaviors of AlN sintered bodies containing 5 wt% of different sizes of MCAS. That of pure AlN is included in the figure for comparison. The addition of micro-MCAS to AlN causes sintering to begin at 1300°C. We attribute this to liquid-phase sintering by the melted MCAS glass, which is presumed to begin formation at its melting point of 1253°C.[22)]

We observe similar behavior with nano-MCAS, although the shrinkage is more severe. Linear shrinkage levels for the AlN samples with nano-, micro-, and no-additive cases are 10.0, 6.8, and 2.0%, respectively. The AlN sample synthesized with the nano-additive exhibits the highest shrinkage. Fig. 3(b) shows the shrinkage rate of the AlN samples with MCAS additive, all of which begin to shrink at 1300°C, regardless of additive size. This is followed by accelerated shrinkage at 1300 - 1600°C. The maximum shrinkage rates occur at 1535°C and 1575°C for the AlN samples with nano- and micro-additives, respectively. This is expected since a finer additive can provide a higher driving force for densification.

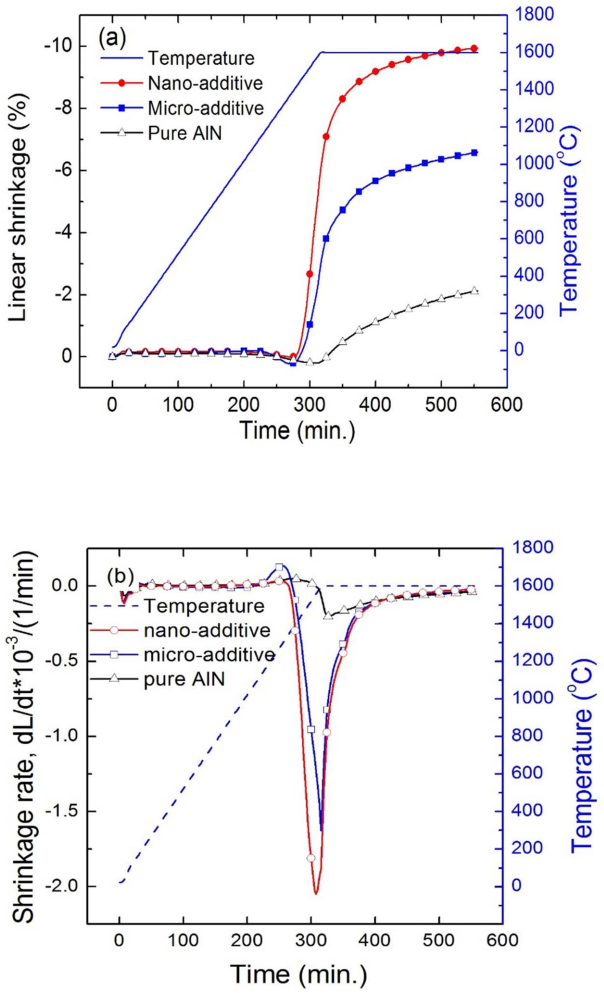

Fig. 3. Changes in (a) shrinkage and (b) shrinkage rate of the pure AlN compact and the AlN compact with 5 wt.% of MCAS additive.

3.2. Sintered density

Figure 4 shows the sintered densities of AlN made with 5 wt% of MCAS under N_2 at different temperatures for 4 h. Pure AlN sintered under the same conditions is included for comparison. The AlN with no additive exhibits a relatively low density even after sintering at 1700°C. The addition of micro-MCAS results in a fast density increase starting at 1400°C, and yields high sintered densities of 96.7, 97.6%, and 98.8% of the theoretical maximum at 1400°C, 1500°C, and 1600°C, respectively.

The addition of nano MCAS results in faster sintering, reaching 89.5% of the theoretical density at 1300°C. This is expected since the finer additive can be distributed more uniformly and can spread AlN particles more quickly, providing enhanced sinterability. We assume that the decreased sintered density at 1700°C is due to the exaggerated grain growth of AlN, which normally traps pores.

3.3. XRD Analysis

Figure 5 shows XRD patterns of the AlN-5 wt% MCAS samples sintered at 1600°C for 4 h in a N_2 atmosphere. As shown in Fig. 5(a), most peaks belong to crystalline AlN, independent of additive size. No new secondary phase is identified, although a very weak peak appears at a 2θ of 34°. We also observe a diffuse halo-like peak at a 2θ of 20°, which normally indicates a noncrystalline phase, which may be melted MCAS.

Figure 5(b) shows the XRD pattern of Fig. 5(a) after removing the main AlN peaks so that the MCAS secondary phase can be observed more clearly. We thus determined that the minor crystalline peak belongs to a Ca-Al compound ($Ca_3Al_{10}O_{18}$), which can form from the interaction and crystallization of CaO and Al_2O_3 from MCAS and Al_2O_3 on

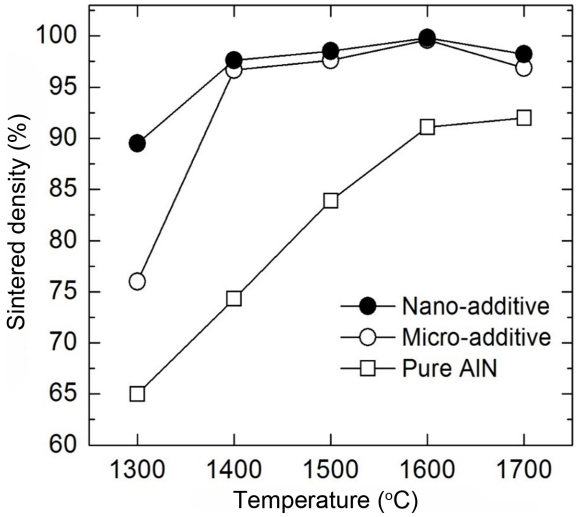

Fig. 4. Sintered density as a function of temperature of the pure AlN and the MCAS-doped AlN (5 wt.%) specimens, sintered for 4 h in a N_2 atmosphere.

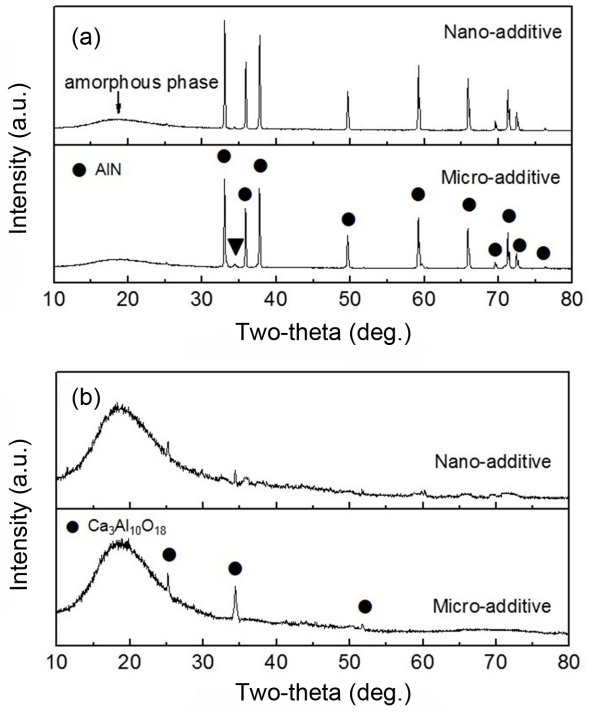

Fig. 5. XRD patterns of the MCAS-doped (5 wt.%) AlN specimens sintered at 1600°C for 4 h; (a) the original pattern and (b) the replotted pattern after deleting AlN peaks.

AlN surfaces. The $Ca_3Al_{10}O_{18}$ phase forms in both MCAS-added samples, although it is more obvious in the micro-additive sample.

It has been well known that polycrystalline additives Y_2O_3 and CaO form liquid phases such as Y-Al or Ca-Al compounds during AlN sintering. This enhances densification by liquid phase sintering, and is followed by crystallization as a secondary phase.[26] In this study, however, the noncrystalline peak in the XRD patterns indicates that the sintering of AlN proceeds with the MCAS liquid via an enhanced mechanism even below 1600°C. This mechanism features MCAS melts and consequent solution-reprecipitation of AlN particles. The MCAS additives provide the same sintering mechanism regardless of their particle sizes.

3.4. Thermal conductivity

Figure 6 shows the thermal conductivities of AlN samples with 5 wt% of MCAS that were sintered at 1600°C for 4 h. The micro- and nano-additives result in thermal conductivities of 32.0 and 82.6 W/mK, respectively, demonstrating that the fine size of the nano-additive significantly enhances the thermal conductivity of AlN. Generally, increasing the amount of lattice oxygen in AlN decreases its thermal conductivity.[14] Y_2O_3 is the most effective AlN additive for densification via liquid phase formation. It also decreases the amounts of oxygen on the AlN surface and in the AlN lattice, producing a thermal conductivity of about 170 W/mK.[11,27]

Pressureless sintering or hot-pressing of polycrystalline

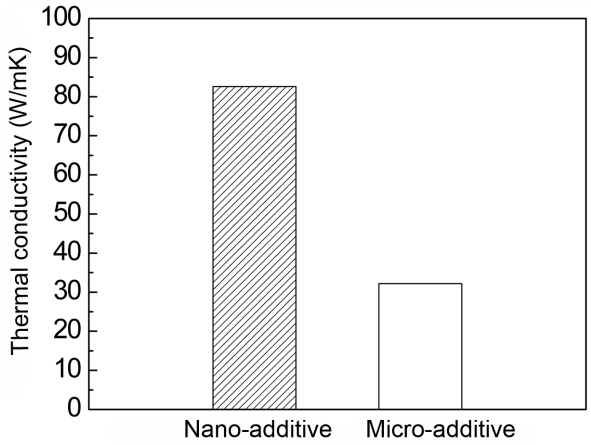

Fig. 6. Thermal conductivity of the MCAS-doped (5 wt.%) AlN specimens sintered at 1600°C for 4 h in a N_2 atmosphere at a heating rate of 5°C/min.

AlN with no additive yielded a thermal conductivity of about 80 W/mK.[28] This value is comparable to that of AlN with nano-MCAS, which is 82.6 W/mK. The results suggest that the nano-MCAS contributes to the low temperature sintering of AlN, but is unable to remove oxygen from the AlN lattice and thus produces a lower thermal conductivity than that of the AlN-Y_2O_3 system. The current most common packaging substrate, Al_2O_3, exhibits a thermal conductivity of only about 20 W/mK. Our thermal conductivity of 82.6 W/mK is high enough to justify considering its replacement with AlN that has been sintered with nano-MCAS additive.

The low thermal conductivity of 32.0 W/mK observed in the case of AlN sintered with micro-MCAS will be discussed during the subsequent microstructure analysis.

3.5. Microstructure analysis

Figure 7 is a back-scattered FE-SEM image of AlN with 5 wt% of nano-MCAS after sintering at 1600°C for 4 h and fracturing to reveal its microstructure. We observe a fully-densified microstructure without any pores. In addition, we verify that AlN exhibits uniform, sharp-edged grains, and identify the MCAS secondary phase distributed along the grain boundaries.

Figure 8 is a back-scattered FE-SEM image of AlN with 5 wt% of the micro-MCAS additive after sintering and fracturing. This microstructure is different from the nano-additive case, as it exhibits non-uniformity and the presence of some pores. In particular, plate-shaped AlN grains form beside the spherical grains that are typical of liquid-phase sintered AlN bodies. These microstructural defects are attributed to unsatisfactory mixing between large micro-MCAS and AlN particles, which results in a considerable decrease in the thermal conductivity.

Baranda *et al.*[29] reported that the addition of 5 wt% of SiO_2 to AlN with 3 wt% of Y_2O_3 decreases its thermal conductivity to 25 W/mK, and claimed that this is attributed to

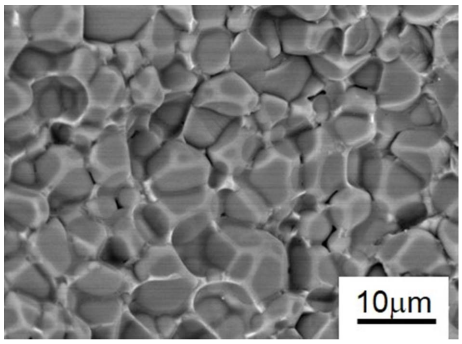

Fig. 7. FE-SEM image of the fracture surface of AlN specimen sintered with 5 wt.% of nano-MCAS additive. Sintering was carried out at 1600°C for 4 h.

microstructural defects created when the AlN lattice incorporates SiO_2 and a polytypoid of SiALON forms. Thus, it is suspected that the plate-shaped grains formed in the micro additive case may be related to SiALON polytypoid[29] or a 27R polytype of AlN,[30] since the SiO_2 contained in the additive can react with AlN.

However, the XRD analysis in Fig. 5 shows no formation of a SiALON phase. Further microstructure analysis via methods such as TEM may be needed to explain the distribution of the MCAS noncrystalline secondary phase in the AlN grains, and to confirm whether the SiALON form is present.

4. Conclusions

In this study, we prepared two sintering additives for the densification of AlN, micro-sized MCAS synthesized via melting and nano-sized MCAS synthesized via the polymeric complex method. By measuring sintering shrinkage, we observed that AlN with 5 wt% of either additive densifies significantly in the 1300 - 1600°C temperature range. More shrinkage was observed when nano-sized MCAS was added. AlN with nano-sized MCAS exhibited its maximum shrinkage rate at 1535°C, which is 40°C lower than that with micro-sized MCAS.

We also confirmed that the sintered densities at various sintering temperatures were higher when nano-MCAS was added. XRD analysis revealed that AlN with 5 wt% of either MCAS additive sintered at 1600°C by forming most of its secondary phase as a noncrystalline phase. We thus determined that the densification of AlN proceeded via a liquid-phase mechanism using melted MCAS.

AlN bodies sintered at 1600°C exhibited thermal conductivities of 82.6 and 32 W/mK with 5 wt% additions of nano- and micro-MCAS, respectively. From these results, we verified that the MCAS particle size is important to the densification and thermal conductivity of AlN. We also concluded that preparing the additive at the nano-scale is an effective method of sintering and enhancing the sintered properties.

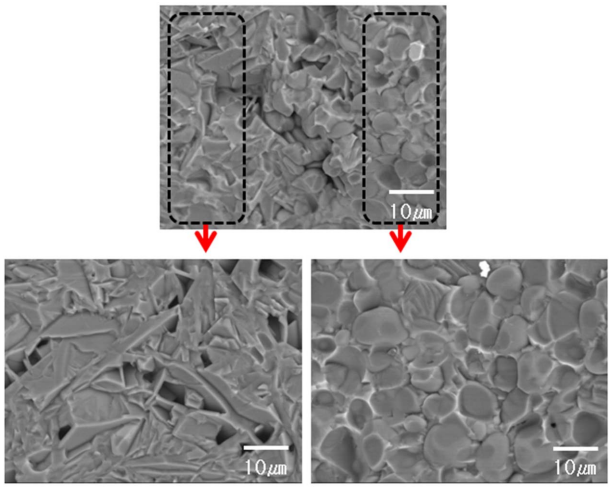

Fig. 8. FE-SEM images for the sintered AlN specimen with 5 wt.% of micro-MCAS additive. Sintering was carried out at 1600°C for 4 h.

Acknowledgments

This research was supported by the Korea Institute for the Advancement of Technology.

REFERENCES

1. Y. Baik and R. A. L. Drew, "Aluminum Nitride: Processing and Applications," *Key Eng. Mater.*, **122-124** 553 (1996).
2. R. E. Simons, "Thermal Management of Electronic Packages," *Solid State Technol.,* **26** [10] 131-37 (1983).
3. C. Zweben, "Adv. Comp. Mater. for Thermal Management in Electronic Packaging," *JOM*, **50** [6] 47-51 (1998).
4. Y. Kurokawa, Z. Utsumi, H. Takamizawa, T. Kamata, and S. Noguchi, "AlN Substrates with High Thermal Conductivity," *IEEE Trans. Comp., Hybrids, Manuf. Technol.*, **8** [2] 247-52 (1985).
5. T. B. Jackson, A. V. Virkar, K. L. More, R. B. Dinwiddie, and R. A. Cutler, "High-Thermal-Conductivity Aluminum Nitride Ceramics: the Effect of Thermodynamic, Kinetic, and Microstructural Factors," *J. Am. Ceram. Soc.,* **80** [6] 1421-35 (1997).
6. A. V. Virkar, T. B. Jackson, and R. A. Cutler, "Thermodynamic and Kinetic Effect of Oxygen Removal on the Thermal Conductivity of Aluminum Nitride," *J. Am. Ceram. Soc.,* **72** [11] 2031-42 (1989).
7. G. A. Slack, "Nonmetallic Crystals with High Thermal Conductivity," *J. Phys. Chem. Solids,* **34** [2] 321-35 (1973).
8. L. M. Sheppard, "Aluminum Nitride: A Versatile but Challenging Material," *Am. Ceram. Soc. Bull.,* **69** [11] 1801-3 (1990).
9. K. Komeya, H. Inoue, and A. Tsuge, "Role of Y_2O_3 and SiO_2 Additions in Sintering of AlN," *J. Am. Ceram. Soc.,* **57** [9] 411 (1974).
10. K. Komeya, A. Tsuge, H. Inoue, and H. Ohta, "Effect of $CaCO_3$ Addition on the Sintering of AlN," *J. Mater. Sci. Lett.,* **1** [8] 325-26 (1982).
11. N. Kuramoto, H. Taniguchi, and I. Aso, "Development of

Translucent Aluminum Nitride Ceramics," *Am. Ceram. Soc. Bull.*, **68** [4] 883-87 (1989).
12. A. L. Molisani, H. N. Yoshimura, H. Goldenstein, and K. Watari, "Effects of $CaCO_3$ Content on the Densification of Aluminum Nitride," *J. Eur. Ceram. Soc.,* **26** [15] 3431-40 (2006).
13. T. B. Troczynski and P. S. Nicholson, "Effect of Additives on the Pressureless Sintering of Aluminum Nitride between 1500°C and 1800°C," *J. Am. Ceram. Soc.,* **72** [8] 1488-91 (1989).
14. E. Treicher, T. Chartier, P. Bosch, M. F. Denanot, and J. Rabier, "Densification and Thermal Conductivity of Low-Sintering-Temperature AlN Materials," *J. Eur. Ceram. Soc.,* **6** [1] 23-9 (1990).
15. J. Jarrige, K. Bouzouita, C. Doradoux, and M. Billy, "A New Method for Fabrication of Dense Aluminium Nitride Bodies at a Temperature as Low as 1600°C," *J. Eur. Ceram. Soc.,* **12** [4] 279-85 (1993).
16. K. Watari, H. J. Hwang, M. Toriyama, and S. Kanzaki, "Effective Sintering Aids for Low-Temperature Sintering of AlN Ceramics," *J. Mater. Res.,***14** [4] 1409-17 (1999).
17. Y. Liu, H. Zhou, L. Qiao, and Y. Wu, "Low-Temperature Sintering of Aluminum Nitride with YF_3-CaF_2 Binary additive," *J. Mater. Sci. Lett.,* **18** [9] 703-4 (1999).
18. L. Qiao, H. Zhou, H. Xue, and S. Wang, "Effect of Y_2O_3 on Low Temperature Sintering and Thermal Conductivity of AlN Ceramics," *J. Eur. Ceram. Soc.,* **23** [1] 61-7 (2003).
19. C. M. Cheng, C. F. Yang, S. H. Lo, and T. S. Tseng, "Sintering $BaTi_4O_9$/$Ba_2Ti_9O_{20}$-Based Ceramics by Glass Addition," *J. Eur. Ceram. Soc.,* **20** [8] 1061-67 (2000).
20. Q. Zhang, G. Jiang, H. Zhuang, W. Li, X. Fu, and D. Yan, "Effects of Gravity on the Microstructure of AlN/Glass Composites," *Mater. Sci. Eng. A,* **352** [1] 217-20 (2003).
21. C. F. Yang, C. M. Cheng, H. H. Chung, and C. C. Chan, "Sintering AlN Ceramics Below 1500°C with MgO-CaO-Al_2O_3-SiO_2 Glass Addition," *Key Eng. Mater.*, **336-338** 1868-71 (2007).
22. H. J. Lee, S. W. Kim, and S. S. Ryu, "Sintering Behavior of Aluminum Nitride Ceramics with MgO–CaO–Al_2O_3–SiO_2 Glass Additive," *Int. J. Refract. Met. Hard Mater.*, **53** 46-50 (2015).
23. H. M. Lee, K. Bharathi, and D. K. Kim, "Processing and Characterization of Aluminum Nitride Ceramics for High Thermal Conductivity," *Adv. Funct. Mater.*, **16** [6] 655-69 (2014).
24. J. Y. Qiu, Y. Hotta, and K. Watari, "Enhancement of Densification and Thermal Conductivity in AlN Ceramics by Addition of Nano-Sized Particles," *J. Am. Ceram. Soc.,* **89** [1] 377-80 (2006).
25. H. J. Lee, W. S. Cho, H. J. Kim, W. Pan, M. Shahid, and S. S. Ryu, "Synthesis of MgO-CaO-Al_2O_3-SiO_2 Nano Powder by Polymeric Complex Method as a Novel Sintering Additive of AlN Ceramics," *Electron. Mater. Lett.,* **12** [6] 732-37 (2016).
26. A. L. Molisani, H. N. Yoshimura, and H. Goldenstein, "Sintering Mechanisms in Aluminum Nitride with Y or Ca-Containing Additive," *J. Mater. Sci.: Mater. Electron.,* **20** [1] 1-8 (2009).
27. A. V. Virkar, T. B. Jackson, and R. A. Cutler, "Thermodynamic and Kinetic Effects of Oxygen Removal on the Thermal Conductivity of Aluminum Nitride," *J. Am. Ceram. Soc.*, **72** [11] 2031-42 (1989).
28. Y. Kurokawa, K. Utsumi, and H. Takamizawa, "Development and Microstructural Characterization of High-Thermal Conductivity Aluminum Nitride Ceramics," *J. Am. Ceram. Soc.,* **71** [7] 588-94 (1988).
29. P. S. De Baranda, A. K. Knudsen, and E. Ruh, "Effect of SiO_2 on the Thermal Conductivity of Aluminum Nitride," *J. Am. Ceram. Soc.*, **76** [7] 1761-71 (1993).
30. T. Yagi, K. Shinozaki, N. Ishizawa, N. Mizutani, and M. Kato, "Effect of Silicon Dioxide on the Thermal Diffusivity of Aluminum Nitride," *J. Am. Ceram. Soc.,* **71** [7] C334-38 (1988).